BIULETYN INSTYTUTU TECHNIKI CIEPLNEJ POLITECHNIKI WARSZAWSKIEJ
Nr 83 1996

Janusz Adamski

Institute of Heat Engineering
Warsaw University of Technology

THE NUCLEAR REACTOR PRESSURE VESSEL AND THERMAL SHIELD ACTIVITY

The results of the analysis of the pressure vessel and thermal shield (n,γ) activity of the PWR (WWER) reactor are presented. It was shown that the saturation activity is reached after six months of the irradiation. Two years after the shut-down of the nuclear reactor the activity drops to the level compared to the natural reactivity of the earth.

INTRODUCTION

The nuclear reactor pressure vessel and thermal shield are working in the field of neutron and gamma flux. After the start-up of the nuclear reactor in a few months they become highly active. The activity of the pressure vessel is due mainly to the (n,γ) reaction. After the shut-down the nuclear power station the activity of the pressure vessel drops. The nuclear reactor core is located in the pressure vessel, hence the vessel is the biggest source of activity compared to the rest of equipment of the primary circuit.

1. ANALYSIS OF THE THERMAL SHIELD AND PRESSURE VESSEL ACTIVITY

The cylindrical pressure vessel and thermal shield have been approximated by plate of the same thickness as the vessel wall. According to this assumption the calculations of the activity have been done for the infinite plate (Fig. 1) [5].

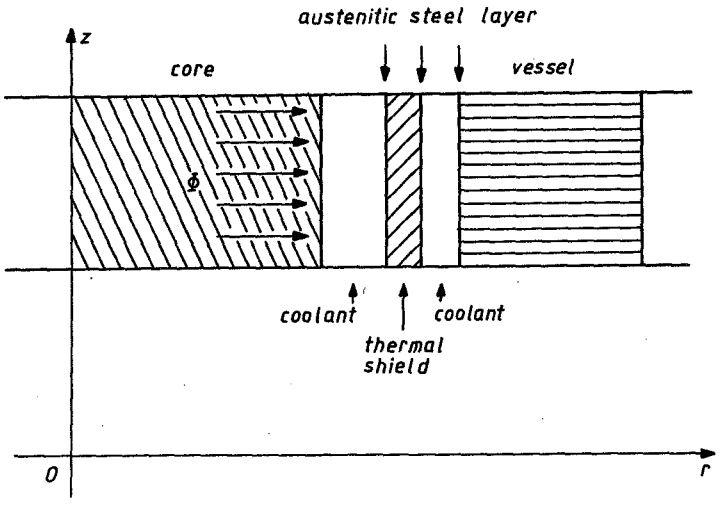

Fig. 1. The cylindrical pressure vessel approximation by a plate

The isotopic content of the steel layer (PN-72/H-84018) is:

C – 0,03%, Cr – 17%, Ni – 12%, Mo – 2,5%, Fe – 68,4%

The isotopic content of the austenitic layer (PN-71/H-86020) is:

C – 0,15%, Mn – 1%, Al – 0,02%, V – 0,1%, Ti – 0,07%, Nb – 0,04%, N – 0,1%, Fe – 98,52%

The physical parameters of the isotopes present in these two material are given in Table 1 and Table 2.

The growth of the activity of the layer is given by the expression

$$A_i(t) = N_{i0}\sigma_{ai}\Phi\left(1 - e^{-\lambda i t}\right); \quad i = 1,2,3,\ldots,n \tag{1}$$

where: Φ – the neutron flux on the inside surface of the layer [$cm^{-2}\cdot s^{-1}$],
i – number of isotope,
N_{i0} – number of atoms of the isotope i in the unit volume of the material for $t = 0$ [$at\cdot cm^{-3}$],
σ_{ai} – microscopic cross section for absorption in the isotope i [b],
λ_i – decay constant [s^{-1}].

It is more convenient to relate the activity to the one ton of the material layer. The volume of the one ton of steel $C = 0{,}127\cdot 10^6$ cm^3 instead of $V = 1$ cm^3 was taken in the calculation. We can write eq.(1) in the form

$$A_i(t) = C\Phi N_{i0}\sigma_{ai}\left(1 - \exp\left(-\lambda_i t\right)\right); \quad i = 1,2,3,\ldots,n. \tag{2}$$

In the calculation the thermal neutron flux of constant value $\Phi = 10^{13}$ $cm^{-2}\cdot s^{-1}$ has been assumed. After certain period the activity of the pressure vessel reaches

the saturation value A_{i0}. After the nuclear reactor shut-down we observe the exponential decay of the activity

$$A_i(t) = A_{i0} \exp(-\lambda_i t); \quad i = 1, 2, 3, \ldots, n \tag{3}$$

Table 1

The parameters of the activated isotopes in the steel layer

Isotope before irradiation	Natural abundance in element [%]	σ_a [b]	Isotope after irradiation	$T_{1/2}$	λ [s^{-1}]	Σ [cm^{-1}]	Radiation energy [MeV]
$_{26}Fe^{58}$	0,33	0,80	$_{26}Fe^{59}$	46,0 d	$1{,}74 \cdot 10^{-7}$	$2{,}12 \cdot 10^{-4}$	1,30
$_{25}Mn^{55}$	100,00	13,40	$_{25}Mn^{56}$	2,6 h	$7{,}40 \cdot 10^{-5}$	$1{,}32 \cdot 10^{-2}$	1,77
$_{13}Al^{27}$	10,00	0,21	$_{13}Al^{28}$	2,3 min	$5{,}02 \cdot 10^{-3}$	$2{,}53 \cdot 10^{-8}$	1,78
$_{23}V^{51}$	99,80	4,50	$_{23}V^{52}$	3,9 min	$2{,}96 \cdot 10^{-3}$	$3{,}02 \cdot 10^{-4}$	1,50
$_{22}Ti^{50}$	5,30	5,30	$_{22}Ti^{51}$	6,0 min	$1{,}93 \cdot 10^{-3}$	$5{,}30 \cdot 10^{-5}$	0,32
$_{41}Nb^{93}$	100,00	100,00	$_{41}Nb^{94}$	6,6 min	$1{,}75 \cdot 10^{-3}$	$2{,}15 \cdot 10^{-5}$	0,04
$_{6}C^{13}$	1,10	3,4 mb	$_{6}C^{14}$	5800 a	$2{,}30 \cdot 10^{-10}$	$4{,}15 \cdot 10^{-9}$	0,16 β^-
$_{7}N^{15}$	0,37	24,00	$_{7}N^{16}$	7,3 s	–	–	–

Table 2

The parameters of the activated isotopes in the austenitic layer

Isotope before irradiation	Natural abundance in element [%]	σ_a [b]	Isotope after irradiation	$T_{1/2}$	λ [s^{-1}]	Σ [cm^{-1}]	Radiation energy [MeV]
$_{26}Fe^{58}$	0,33	0,80	$_{26}Fe^{59}$	46 d	$1{,}74 \cdot 10^{-7}$	$1{,}47 \cdot 10^{-4}$	1,30
$_{24}Cr^{50}$	4,40	16,00	$_{24}Cr^{51}$	27 d	$2{,}97 \cdot 10^{-7}$	$9{,}98 \cdot 10^{-3}$	0,32
$_{28}Ni^{64}$	1,90	3,00	$_{28}Ni^{65}$	2,5 h	$7{,}70 \cdot 10^{-5}$	$5{,}73 \cdot 10^{-4}$	0,93
$_{42}Mo^{98}$	23,80	0,13	$_{42}Mo^{99}$	67 h	$2{,}87 \cdot 10^{-6}$	$4{,}85 \cdot 10^{-5}$	0,84
$_{6}C^{13}$	1,10	3,5 mb	$_{6}C^{14}$	5800 a	$2{,}30 \cdot 10^{-10}$	$3{,}86 \cdot 10^{-9}$	0,16 β^-

2. RESULTS AND DISCUSSION

The calculations of the activity have been done for the steel layer of the thickness H = 14 cm and for the austenitic – stainless steel layer of the thickness H = 0,6 cm. In the first step the thermal neutron flux $\Phi_0 = 10^{13}$ cm^{-2}·s^{-1} has been assumed. In the second step one group fast flux 0,4 MeV and $\Phi_0 = 10^{10}$ cm^{-2}·s^{-1} has been assumed. The activation cross section of iron $_{26}Fe^{58}$ (Fig. 9), and other isotopes present in the alloys obey „1/v law", hence the activity from the fast part of the neutron flux is 10^6 times smaller than from the thermal part.

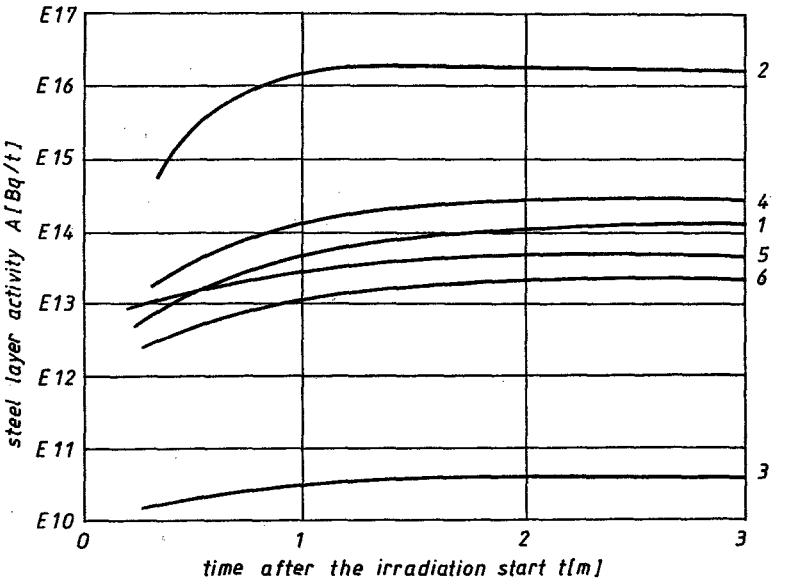

Fig. 2. The steel layer activity growth after the start-up of the nuclear reactor. $\Phi_0 = 10^{13}$ cm^{-2}·s^{-1}, H = 14 cm, 1 – $_{26}Fe^{59}$, 2 – $_{25}Mn^{56}$, 3 – $_{13}Al^{28}$, 4 – $_{23}V^{52}$, 5 – $_{22}Ti^{51}$, 6 – $_{41}Nb^{94}$

The activity is proportional to the flux magnitude. In these calculations constant thermal flux $\Phi_0 = 10^{13}$ cm^{-2}·s^{-1} has been assumed in the shield, i.e. the value of the flux in the reactor core, which is a very conservative assumption. Hence, the presented results of the analysis are too pessimistic. The saturation activity is proportional to the steel layer and stainless steel cladding thickness (Fig. 6). It takes place after six months of the irradiation start-up and reaches 10^{16} Bq·t^{-1} (Fig. 3). The greater part of the steel activity is given by $_{25}Mn^{56}$ (Fig. 3). The smallest part to the activity $3 \cdot 10^{10}$ Bq·t^{-1} is given by $_{13}Al^{28}$. The values of the saturation activity of vanadium, iron, titanium and

niobium are in between (Fig. 2). As it can be seen, the activity of one ton of the reactor vessel equals the activity of 0,3 ton of radium. After the shut-down of the nuclear reactor the activity of the nuclear power station primary coolant circuit drops. The activity of aluminium, $_{13}Al^{28}$, vanadium $_{23}V^{52}$, titanium $_{22}Ti^{51}$ and niobium $_{41}Nb^{94}$ becomes negligible after few hours. The activity of manganese $_{25}Mn^{56}$ becomes negligible after several hours (Fig. 4). The iron $_{26}Fe^{59}$ activity drops to the level 10^{10} Bq·t^{-1} after two years of cooling (Fig. 5).

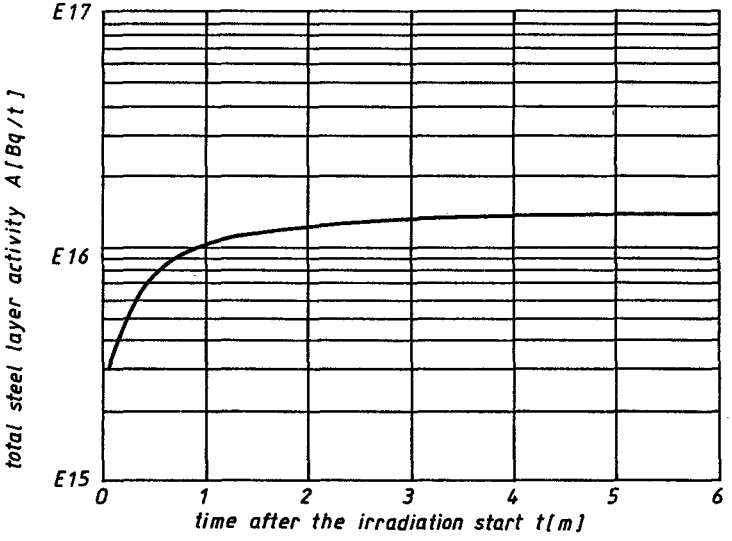

Fig. 3. The total activity of the steel layer after the start-up of the nuclear reactor; $\Phi_0 = 10^{13}$ cm^{-2}·s^{-1}, $H = 14$ cm

The saturation activity of the stainless steel cladding occurs after a few months of the irradiation start-up and reaches 10^{16} Bq·t^{-1} (Fig. 7). The greater part to the cladding activity is given by $_{24}Cr^{51}$ and the smallest part is given by $_{42}Mo^{99}$. After the nuclear reactor shut-down the activity of the stainless steel cladding drops to the level 10^{11} Bq·t^{-1} after two years of cooling (Fig. 8). The activity of nickel $_{28}Ni^{65}$ and molybdenum $_{42}Mo^{99}$ becomes negligible in a few hours. The activity of chromium $_{24}Cr^{51}$ drops to the level 10^{8} Bq·t^{-1} after three years of cooling and the activity of iron $_{26}Fe^{59}$ to the same level after five years after the nuclear reactor shut-down.

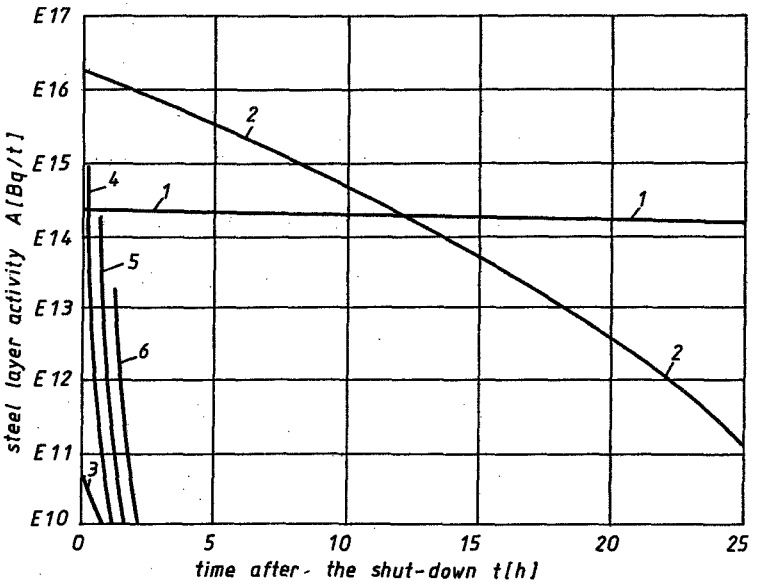

Fig. 4. The steel layer activity drop after the shut-down of the nuclear reactor; $\Phi_0 = 10^{13}$ cm$^{-2}\cdot$s^{-1}, $H = 14$ cm, 1 – $_{26}Fe^{59}$, 2 – $_{25}Mn^{56}$, 3 – $_{13}Al^{28}$, 4 – $_{23}V^{52}$, 5 – $_{22}Ti^{51}$, 6 – $_{41}Nb^{94}$

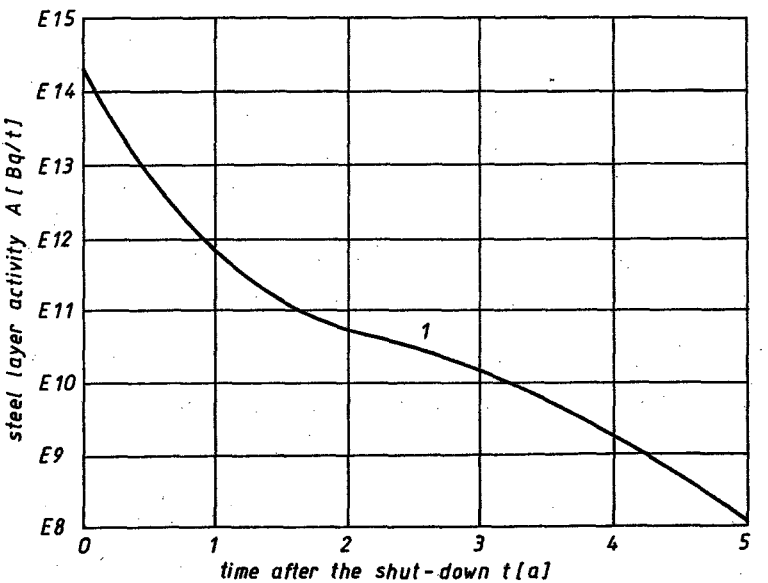

Fig. 5. The steel layer activity drop after the shut-down of the nuclear reactor; $\Phi_0 = 10^{13}$ cm$^{-2}\cdot$s^{-1}, $H = 14$ cm, 1 – $_{26}Fe^{59}$

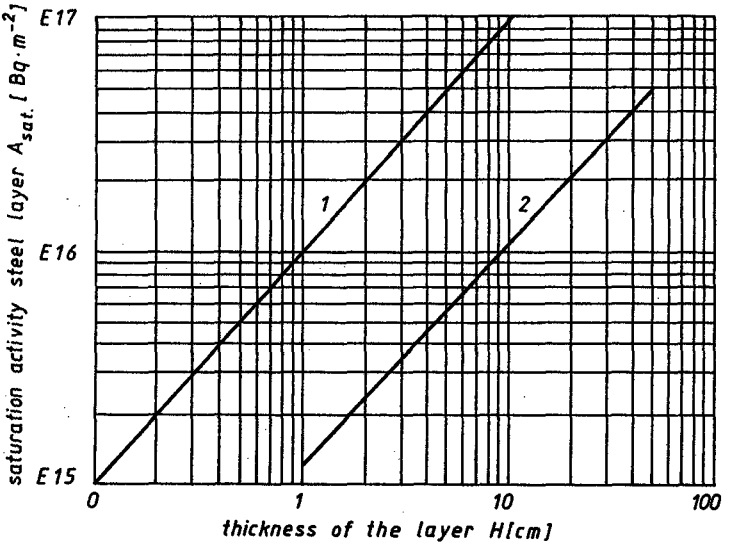

Fig. 6. The saturation activity of the steel as a function of the layer thickness; 1 – the austenitic (stainless) steel, 2 – the construction steel (vessel and thermal shield), $\Phi_0 = 10^{13}$ $cm^{-2} \cdot s^{-1}$

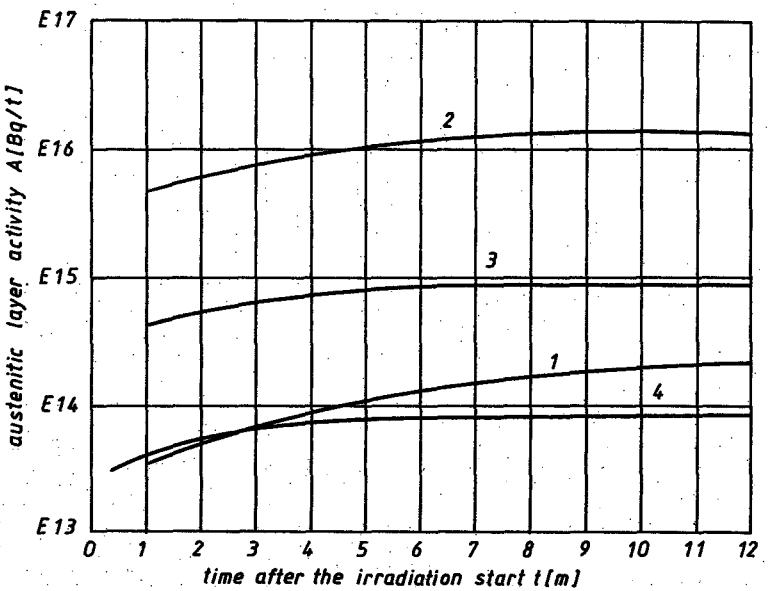

Fig. 7. The austenitic layer activity growth after the start-up of the nuclear reactor; $\Phi_0 = 10^{13}$ $cm^{-2} \cdot s^{-1}$, H = 0,6 cm, 1 – $_{26}Fe^{59}$, 2 – $_{24}Cr^{51}$, 3 – $_{28}Ni^{65}$, 4 – $_{42}Mo^{99}$

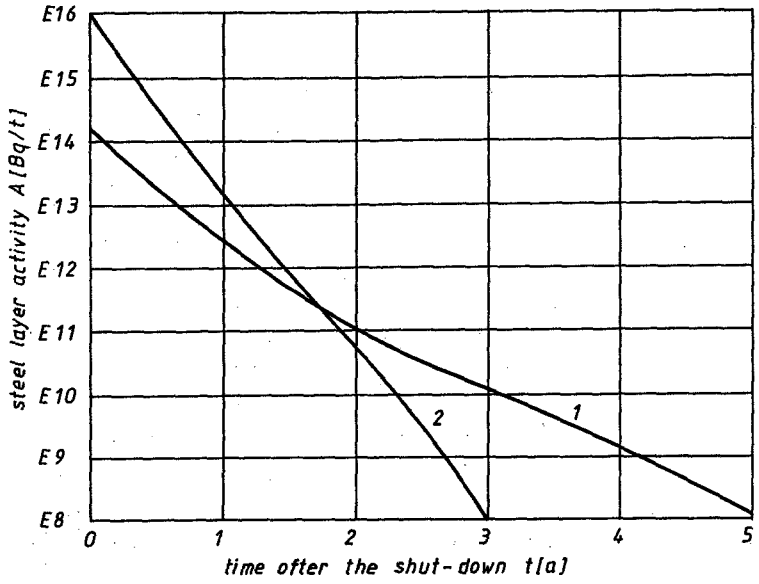

Fig. 8. The austenitic layer activity drop after the shut-down of the nuclear reactor; $\Phi_0 = 10^{13}$ cm$^{-2}\cdot$s^{-1}, H = 0,6 cm, 1 – $_{26}Fe^{59}$, 2 – $_{24}Cr^{51}$

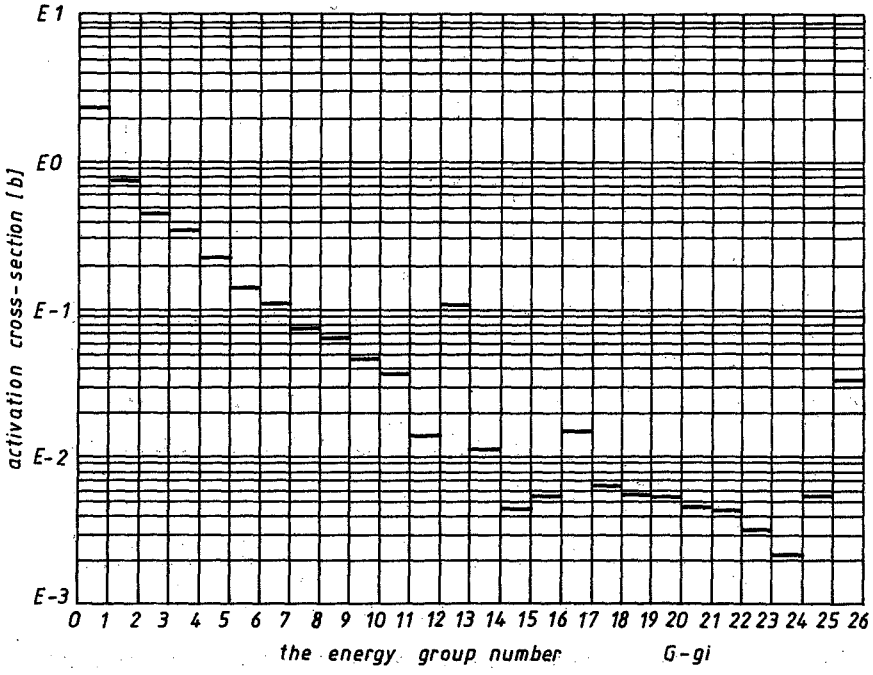

Fig. 9. Iron-58 activation cross-section

3. CONCLUSIONS

The saturation activity is reached in the steel pressure vessel and thermal shield after six months of the nuclear reactor start-up and equals 10^{16} Bq·t^{-1}. The greater part to the activity of the steel is given by $_{25}Mn^{56}$. It is gamma activity of 1,77 MeV with $T_{1/2}$ = 2,6 h. Similar saturation activity is reached by the austenitic layer after three months of irradiation. The greater part to the activity of the austenitic layer is given by $_{24}Cr^{51}$. It is gamma activity of 0,32 MeV with $T_{1/2}$ = 27 d. After the nuclear reactor shut-down the activity of the pressure vessel drops and in two years of cooling reaches 10^{10} Bq·t^{-1}. The natural uranium radioactivity equals $1{,}7 \cdot 10^{11}$ Bq·t^{-1} and the natural radioactivity of the earth equals 10^{6} Bq·t^{-1} [3].

One should remember that the reactor core is located in the pressure vessel, hence the vessel is the biggest source of activity compared to the rest of equipment of the nuclear power station primary coolant circuit.

REFERENCES

1. Л.П. Абагян, Н.О. Базазянц, И.И. Бондаренко, М.Н. Николаев: *Групповые константы для пасчета ядерных реакторов.* Атомиздат, Москва 1964.
2. E. Browne, R. Firestone: *Table of radioactive isotopes.* J. Wiley Interscience Publ., N.York 1986.
3. A. Ciszewski, T. Radomski, A. Szummer: *Materiałoznawstwo.* OWPW, Warszawa 1996.
4. D.J. Hughes: *Neutron cross-sections.* BNL-325 plus supplements.
5. F.J. Rahn: *A guide to nuclear power technology.* J. Wiley & Sons, 1984.
6. T. Tamura, T. Tachibana, T. Horiguchi: *Chart of the nuclides.* Japan Atomic Energy Research Institute, 1992.

WZROST I ZANIK AKTYWNOŚCI ZBIORNIKA CIŚNIENIOWEGO REAKTORA JĄDROWEGO

Streszczenie

Badano, po jakim czasie można przystąpić do demontażu urządzeń obiegu pierwotnego wodno ciśnieniowego reaktora jądrowego w wyłączonej elektrowni jądrowej. Przedstawiono wyniki analizy wzrostu i zaniku aktywności zbiornika i osłony termicznej. Obliczenia wykonano dla różnych wartości grubości ścian i warstwy platerowanej. Uwzględniono reakcję (n,γ) i dwie grupy neutronów, termiczną i prędką 0,4 MeV. Największy wkład w aktywację stali konstrukcyjnej zbiornika i osłony termicznej ma izotop manganu o liczbie masowej 55. W wyniku reakcji (n,γ) powstaje promieniotwórczy mangan 56 o okresie półrozpadu 2,6 h i energii kwan-

tów gamma 1,77 MeV. Aktywność nasycenia wynosi 10^{16} Bq·t^{-1}. Osiągana jest po sześciu miesiącach pracy reaktora. Podobną wartość ma aktywność nasycenia warstwy platerowanej osiągana po 3 miesiącach napromieniowania. Największy wkład w aktywację ma izotop chromu-50. Powstaje chrom 51 o okresie półrozpadu 27 dni i energii kwantów gamma 0,32 MeV. Po wyłączeniu reaktora aktywnść zbiornika i osłony termicznej spada w ciągu 2 lat do około 10^{10} Bq·t^{-1}. Jest to aktywność porównywalna z naturalną aktywnością gleby.

АКТИВАЦИЯ И ЗАТУХАНИЕ КОРПУСА ЯДЕРНОГО РЕАКТОРА ПОД ДАВЛЕНИЕМ

Краткое содержание

Б работе проведены исследования, через какое время можно приступить к демонтажу оборудования первого контура водо-водяного энергетического ядерного реактора. Представлены результаты расчетов роста и затухания активности корпуса и тепловой защиты водо-водяного реактора в результате реакции (n,γ). Приняты во внимание две группы нейтронов: тепловые и быстрые 0,4 МеВ. Показано, что самый большой вклад в активацию корпуса после запуска ядерного реактора вносит изотоп манганец-55. В результате реакции (n,γ) образуется гамма радиоактивный манганец-56 ($T_{1/2}$ = 2,6 ч и гамма 1,77 МеВ).

Через шесть месяцев работы реактора активность составляет 10^{16} Eq·t^{-1}, а через три месяца активность наплавки имеет ту самую стоимость. Показано, что наибольший вклад в активирование наплавки вносит изотоп хрома-Cr51. В результате реакции (n,γ) образуется гамма радиоактивный изотоп хрома-Cr51. Содержание хрома в сплавах стали равно 17%. Из этих семнадцати процентов хрома 4,4% составляет изотоп Cr50, который активируется. После остановки реактора активность корпуса и тепловой защиты снижается в течение двух лет до 10^{10} Eq·t^{-1}. Эта активность равна активности земли.

Appendix

THE NEUTRON FLUX

Let us consider the first case where attenuation of the flux in the layer is due to the absorption. The thermal flux in the layer $\Phi_2(x)$ is given by the expression [2]

$$\Phi_2(x) = \Phi_{20} \exp\left(-\left(\sum_i N_{i0}\sigma_{ai}\right)x\right) \tag{1}$$

The attenuation of the thermal flux in the thermal shield and pressure vessel is shown on the Fig. 3 and Fig. 4.

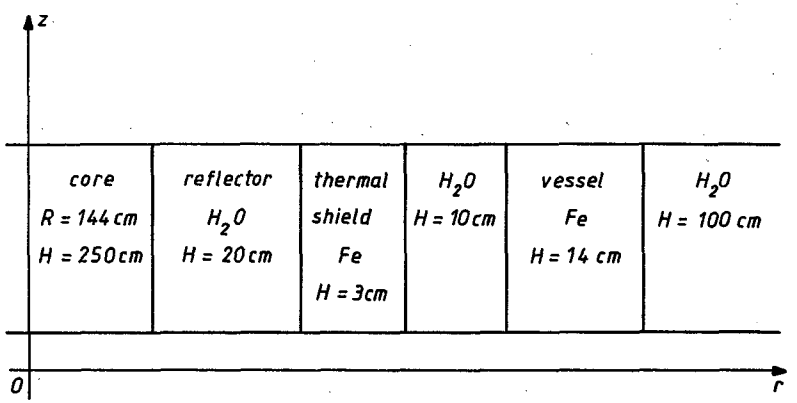

Fig. 1. WWER-440 type reactor approximation layers thickness

Let us consider the second case where diffusion and slowing down of neutron are taken into acount. Let us assume WWER-440 type reactor (Fig. 1). The thermal neutron flux $\Phi_2(x)$ resulting from fast neutron plane source Φ_1 [$cm^{-2} \cdot s^{-1}$] is given by the exppression [2]

$$\Phi_2(x) = \frac{\Phi_1 L_2 e^{\tau_2/L_2}}{4\bar{D}_2}\left(e^{-x/L_2}\left(1 + \operatorname{erf}\left(\frac{x}{(2\tau_2)^{1/2}} - \frac{(\tau_2)^{1/2}}{L_2}\right)\right) + \right.$$
$$\left. + e^{x/L_2}\left(1 - \operatorname{erf}\left(\frac{x}{(2\tau_2)^{1/2}} + \frac{(\tau_2)^{1/2}}{L_2}\right)\right)\right) \tag{2}$$

The two group flux (diffusion theory) $\Phi_1(x)$ and $\Phi_2(x)$ in the reactor core is shown in the Fig. 2. The thermal flux (diffusion and slowing down theory) $\Phi_2(x)$ in the layers is shown in Figs. 3, 4 and 5. The thermal absorption flux in the thermal shield and vessel is greater than fast source (diffusion and slowing down theory) thermal flux. Hence, in the first approximation the flux of constant value has been taken in the calculations.

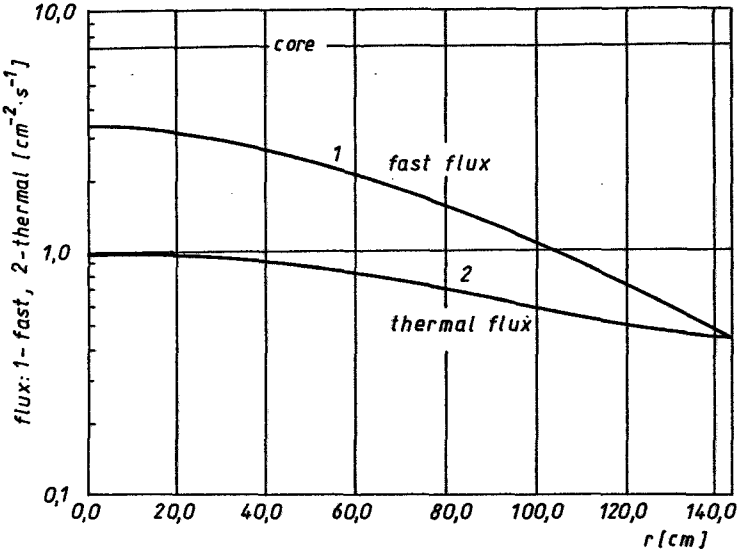

Fig. 2. The two group flux in the PWR reactor core; R = 144 cm, H = 250 cm, reflector H_2O, T = 20 cm

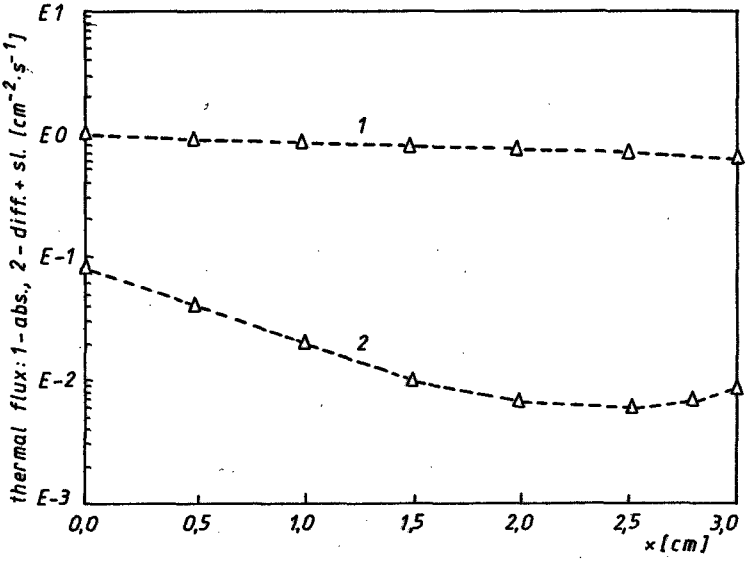

Fig. 3. Thermal flux $\Phi_2(x)$ in the thermal shield WWER-440 type reactor; 1 – absorption (eq.1), 2 – diffusion and slowing down (eq.2)

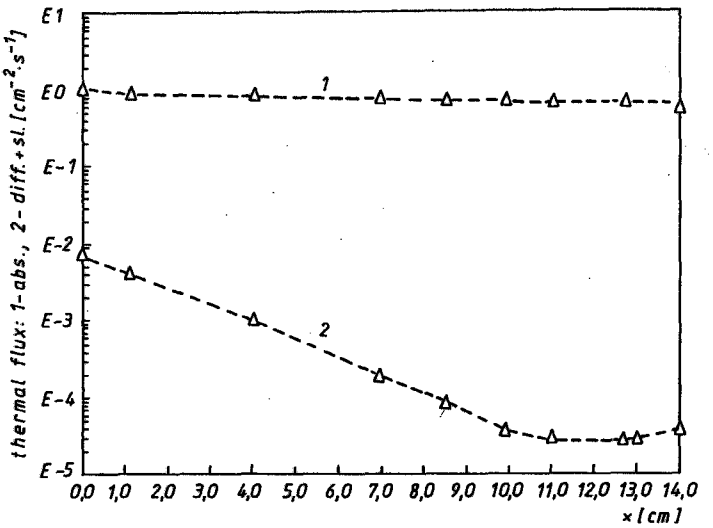

Fig. 4. Thermal flux $\Phi_2(x)$ in the vessel WWER-440 type reactor; 1 – absorption (eq.1), 2 – diffusion and slowing down (eq.2)

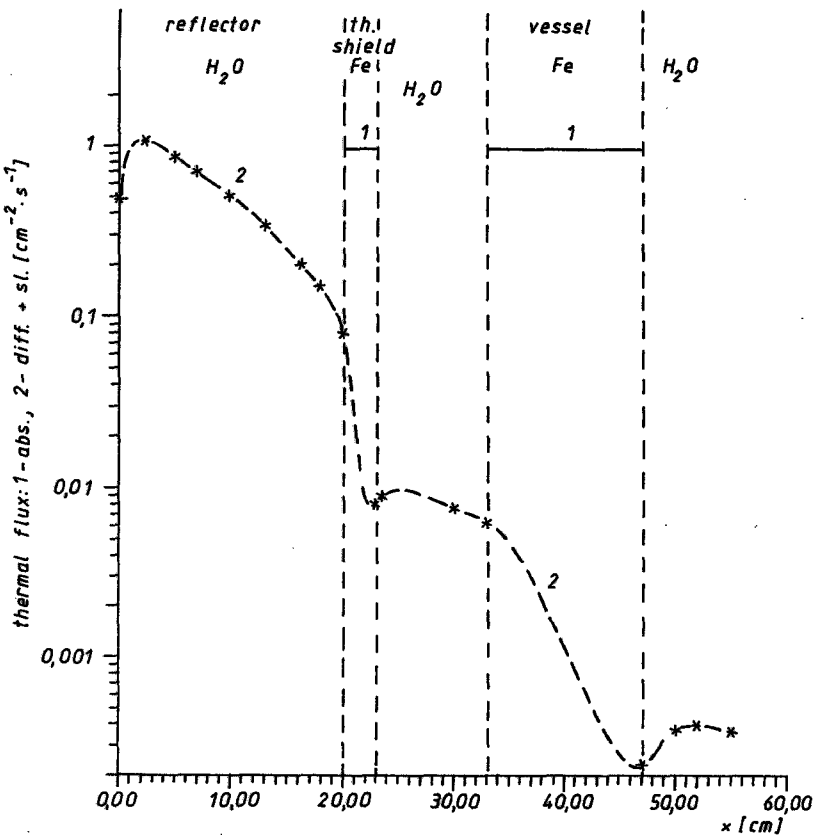

Fig. 5. Thermal flux $\Phi_2(x)$ in the layers. WWER-440 type reactor approximation (eq.1) and (eq.2)

REFERENCES

1. ANL-5800 Reactor Physics Constants, USAEC, 1963.
2. J.R. Lamarsh: *Introduction to nuclear reactor theory.* Addison Wesley Publ. Company, 1972.
3. W. Łukaszek: *Podstawy obliczania osłon przed promieniowaniem jądrowym.* Wyd. Politechniki Śląskiej Nr 1723, Gliwice 1993.
4. W.H. Press: *Numerical Recipes.* Cambridge University Press, Cambridge 1986.